AD-A195 397 METALLURGICAL EXAMINATION OF A DIAPHRAGM - LOCKUP CLUTCH PISTON(U) ARMY LAB COMMAND WATERTOWN MA MATERIAL TECHNOLOGY LAB V K CHAMPAGNE APR 88 MTL-TR-88-6

1/1

UNCLASSIFIED F/G 13/9 NL

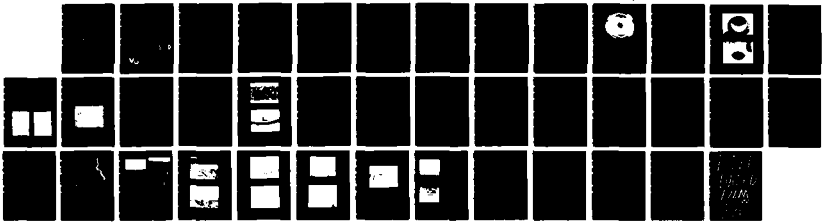

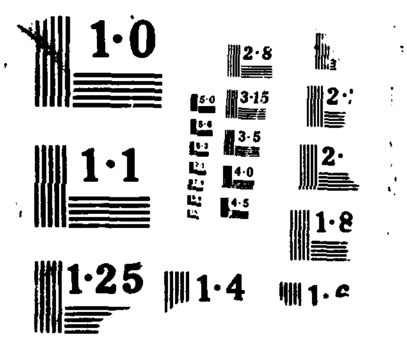
1·0
2·8
3·15
3·5
4·0
4·5
1·1
1·8
1·25
1·4

DTIC FILE COPY

MTL TR 88-6

AD

AD-A195 397

METALLURGICAL EXAMINATION OF A DIAPHRAGM - LOCKUP CLUTCH PISTON

VICTOR K. CHAMPAGNE, Jr.

MATERIALS TESTING AND EVALUATION BRANCH

April 1988

Approved for public release; distribution unlimited.

US ARMY
LABORATORY COMMAND
MATERIALS TECHNOLOGY LABORATORY

U.S. ARMY MATERIALS TECHNOLOGY LABORATORY
Watertown, Massachusetts 02172-0001

UNCLASSIFIED

SECURITY CLASSIFICATION OF THIS PAGE (When Data Entered)

REPORT DOCUMENTATION PAGE		READ INSTRUCTIONS BEFORE COMPLETING FORM
1. REPORT NUMBER MTL TR 88-6	2. GOVT ACCESSION NO.	3. RECIPIENT'S CATALOG NUMBER
4. TITLE (and Subtitle) METALLURGICAL EXAMINATION OF A DIAPHRAGM - LOCKUP CLUTCH PISTON		5. TYPE OF REPORT & PERIOD COVERED Final Report
		6. PERFORMING ORG. REPORT NUMBER
7. AUTHOR(s) Victor K. Champagne, Jr.		8. CONTRACT OR GRANT NUMBER(s)
9. PERFORMING ORGANIZATION NAME AND ADDRESS U.S. Army Materials Technology Laboratory Watertown, Massachusetts 02172-0001 ATTN: SLCMT-MRM		10. PROGRAM ELEMENT, PROJECT, TASK AREA & WORK UNIT NUMBERS
11. CONTROLLING OFFICE NAME AND ADDRESS U.S. Army Laboratory Command 2800 Powder Mill Road Adelphi, Maryland 20783-1145		12. REPORT DATE April 1988
		13. NUMBER OF PAGES 33
14. MONITORING AGENCY NAME & ADDRESS (if different from Controlling Office)		15. SECURITY CLASS (of this report) Unclassified
		15a. DECLASSIFICATION DOWNGRADING SCHEDULE

16. DISTRIBUTION STATEMENT (of this Report)

Approved for public release; distribution unlimited.

17. DISTRIBUTION STATEMENT (of the abstract entered in Block 20, if different from Report)

18. SUPPLEMENTARY NOTES

19. KEY WORDS (Continue on reverse side if necessary and identify by block number)

Clutch pistons, High carbon steels, Failure, Scanning electron microscopy (SEM), Metallography

20. ABSTRACT (Continue on reverse side if necessary and identify by block number)

(SEE REVERSE SIDE)

DD FORM 1 JAN 73 1473 EDITION OF 1 NOV 65 IS OBSOLETE

UNCLASSIFIED

SECURITY CLASSIFICATION OF THIS PAGE (When Data Entered)

Block No. 20

ABSTRACT

A metallurgical examination was performed on a diaphragm - lockup clutch piston which experienced cracking around the inside diameter. The study required reviewing the manufacturing procedures, analyzing the service conditions and determining the operating stresses induced on the part in service.

The extent of cracking was verified by using magnetic particle testing. Material identification and characterization was accomplished by performing mechanical testing, chemical analysis, and metallographic techniques. Scanning electron microscopy (SEM) and electron dispersive spectroscopy (EDS) was used to examine features of the material and the fracture surface. Finally, a mechanics analysis was included in order to calculate an approximation of the actual operating stresses, the critical stress-intensity factor (K_{IC}) for the material, the stress-intensity factor (K_I) under observed conditions, and the possible crack propagation rates under actual loading. Measurements of the residual stress were also taken utilizing X-ray diffraction.

CONTENTS

Page

INTRODUCTION. 1

MODE OF OPERATION 1

SEQUENCE OF MANUFACTURING OPERATIONS. 2

NONDESTRUCTIVE INSPECTION 5

MATERIAL EXAMINATION. 5

MICROSTRUCTURE. 7

HARDNESS MEASUREMENTS 7

VISUAL EXAMINATION. 10

SCANNING ELECTRON MICROSCOPY/ENERGY DISPERSIVE SPECTROSCOPY 10

MECHANICS ANALYSIS

Methods. 15

RESULTS OF THE MECHANICS ANALYSIS 19

DISCUSSION. 19

CONCLUSIONS 21

ACKNOWLEDGMENT. 21

INTRODUCTION

The main purpose of this study was to determine if TACOM reference P/N 6769139, Diaphragm - Lockup Clutch Piston, could be placed back into service after circumferential cracks were discovered adjacent to the inside diameter region of the part, during an inspection procedure. A metallurgical investigation was conducted isolating the possible causes of these cracks and a determination was then made as to the affect that these discontinuities had on the functionability of the diaphragm. Thereafter, a recommendation was rendered concluding whether or not this part could be placed back into service without risk of subsequent failure.

The cracks were first observed by inspectors at Anniston Army Depot during an overhaul inspection procedure, reference OIP 8356940 - TACOM DMWR9 - 2520 - 249. They were revealed using the flourescent magnetic particle testing method. The diaphragm, like many others used in the field, had been in operation prior to this inspection and was currently in storage waiting to be placed back into service. The exact length of time that the part had been in service and in storage was unknown. However, it was revealed by the manufacturer (and later confirmed by chemical analysis) that the base material used in the fabrication of this particular lot was SAE 1074 steel. It is important to note at this time that the base material had been changed to SAE 6150 steel during 1980 and 1981 because of failures which were believed to be material related. This information indicated that the part under examination was at least six to seven years old and could be in the order of twenty years old, as indicated by the manufacturer and also by dated engineering drawings.

Engineering drawings and all appropriate supporting documentation describing the history of the part, its means of operation, and other technical information were furnished by Mr. Brian Rich - Mechanical Engineer, Anniston Army Depot, Anniston, AL.

The sequence of manufacturing operations, as well as information concerning material processing and design considerations were furnished by the supplier and manufacturer of the diaphragm.

Supplier	Manufacturer
Detroit Diesel Allison	E.C. Styberg, Engineering
P.O. Box 894	P.O. Box 788
Indianapolis, Indiana	Racine, Wisconsin
P.O.C.: Mr. Arf Kheiri	P.O.C.: Mr. John Baker.

MODE OF OPERATION

The converter pump cover assembly (Figure 1, Item 5) is a pressed steel assembly with six drive studs at the front to attach it to the engine flex-drive plates. The rear ends of these six studs enter blind holes in the lockup clutch piston assembly (Item 11) causing the cover and piston to rotate as a unit. A center hub enters the end of the engine crankshaft for alignment. Lockup clutch oil pressure applied between the piston and cover, moves the piston against the lockup clutch disk for clutch application.

Actual operating temperatures of the lockup clutch piston assembly have been measured while the engine was functioning at its highest capacity. Temperatures exceeding 300°F (149°C) have been recorded. Simultaneously, corresponding oil pressures were also measured. Oil pressures within the assembly have reached 180 psi.

SEQUENCE OF MANUFACTURING OPERATIONS

The following information was furnished by E. C. Styberg Engineering Co., Inc. The part was manufactured for Detroit Diesel Allison who in turn supplied these parts to the Department of the Army (see Figure 2).

1. Stock material consisting of SAE 1074 steel is subjected to an annealing process. This heat treating procedure is designed to impart softness and ductility into the workpiece for easier subsequent machining and further material processing. E. C. Styberg Engineering Co., received the workpiece in this condition.

2. The workpiece is subjected to a "piercing" operation which forms the outside diameter (A) by upsetting the material through the use of piercing tools. This procedure is performed at room temperature.

3. The diaphragm is then "drawn" which is a cold-working operation in which the geometrical configuration of the part is formed through the use of a press and a die.

4. The inside diameter (B) of the part is "blanked" downward with the part coned up. This is a punching operation performed at room temperature. The inside diameter size checks to 2.124 inches.

5. The outside diameter (A) is then "trimmed" which is a procedure designed to shear excess flash from the main body of the part. A trimming press forces a die, against the diaphragm, having a cutting edge shaped to the contour of the part. This is also performed at room temperature.

6. The diaphragm undergoes an austenitizing heat treating procedure. The austenitizing temperature is 1500°F.

7. The part is now hardened and strengthened by quenching. The quenching media is oil.

8. A tempering treatment is then performed at 750°F and is followed by air cooling.

9. A magnetic particle test is now performed on the diaphragm to reveal any discontinuties which may have been the result of prior material processing. A 25 percent representative sample size is inspected.

10. The part is then shot peened to induce compressive stresses into the exposed surface.

11. The inside diameter (B) is machined to allowable tolerances using carbide inserts while the outside diameter (A) is ground down to size. A cooling fluid is utilized with these procedures.

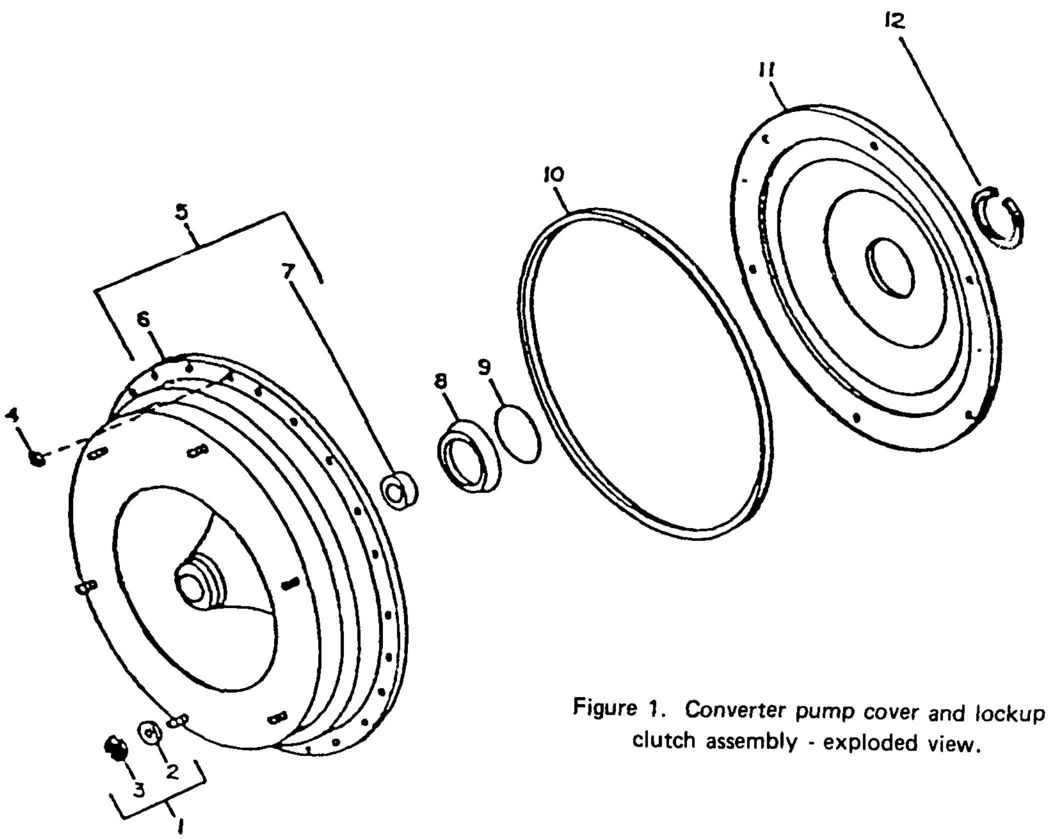

Figure 1. Converter pump cover and lockup clutch assembly - exploded view.

Table 1. LIST OF COMPONENT PARTS FOR CONVERTER PUMP AND LOCKUP CLUTCH ASSEMBLY

1. Converter stack control spacer kit
2. Spacer:
   0.027 to 0.029 (as-required)
   0.045 to 0.047 (as-required)
   0.063 to 0.065 (as-required)
   0.081 to 0.083 (as-required)
   0.099 to 0.101 (as-required)
3. Retainer
4. Self-locking hexagon nut 5/16-24 (24)
5. Converter pump cover assembly
6. Cover
7. Torque converter cover hub inner Teflon seal ring
8. Converter lockup clutch piston seal retainer
9. Converter lockup clutch piston preformed packing
10. Lockup clutch piston outer seal ring

*11. Lockup clutch piston assembly (diaphragm)

12. Lockup clutch piston retaining ring

*Denotes the part under investigation

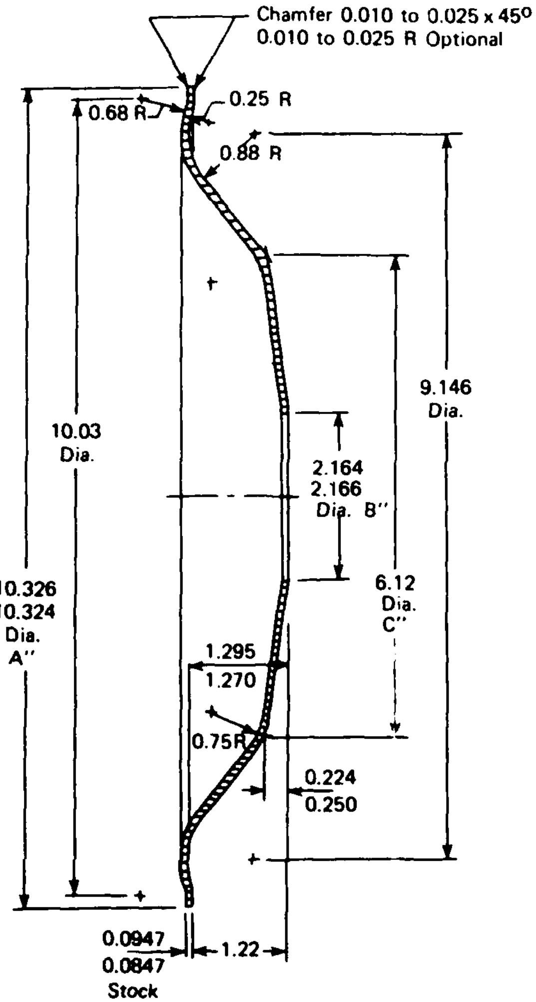

Figure 2. Shows the dimensional schematic of the part and a macrograph in an as-received condition.

NONDESTRUCTIVE INSPECTION

A flourescent magnetic particle test was performed on three of the diaphragms to verify the existence of indications within the inside diameter region. The test revealed evidence of cracking which occurred along the circumference of the inside diameter. Blacklight photography was used to obtain a permanent record of the test. Figures 3 and 4 represent recorded results of two of the inspections performed. The cracks, as shown in these blacklight macrographs, originate from the inside diameter and extend radially outward. It is important to note that these cracks were found only on the convex side of all of the diaphragms tested. There was no evidence of any indications on the concave side of the parts. The cracks on all of the diaphragms did not appear to extend more than approximately a quarter of an inch away from the edge of the inside diameter.

The only comparable differences observed between the three diaphragms which were tested were the number of cracks found per unit area and the arrangement of these cracks. The diaphragm shown in Figure 3 contains an extensive number of cracks, which completely surround and are evenly distributed around the convex side of the inside diameter. The diaphragm shown in Figure 4 differs in that it contains fewer cracks which occur in groups. The third diaphragm tested resembled that of Figure 3.

All diaphragms tested contained cracks which extended radially from the edge of the inside diameter, as well as cracks which originated some small distance away from this area, as shown in Figures 3 and 4. The test also revealed a thin, sharp, indication circumvallating the entire inside diameter. This ring-like feature can be observed more clearly in Figure 3. This indication was attributed to mechanical wear caused by the lockup clutch piston retaining ring (see Figure 1, Item 12).

MATERIAL EXAMINATION

The chemical composition of the SAE 1074 steel is given in Table 2. Typical ranges for this material, taken from the American Society for Metals Handbook, Volume 1, have been included for comparative purposes.[1] The compositional ranges of the material under investigation compare favorably with published values.

Table 2. COMPARISON OF CHEMISTRIES

	Chemical Compositon (Weight Percent)			
Element	C	Mn	Pmax	Smax
ASM Handbook	0.70-0.80	0.50-0.80	0.040	0.050
Diaphragm	0.730	0.720	0.010	0.020

1. *Classification and Designations of Carbon and Alloy Steels.* ASM Metals Handbook, Properties and Selection: Iron and Steel, v. 1, 1978, p. 125.

Figure 3. Blacklight macrograph showing indications revealed by magnetic particle inspection.

Figure 4. Blacklight macrograph of a different diaphragm showing fewer indications which tend to occur in groups.

MICROSTRUCTURE

Figure 5 is a schematic illustrating the areas where metallographic specimens were sectioned from the inside diameter region of the diaphragm. These samples were polished and etched to reveal the microstructural features of the material. Figures 6 and 7 are transverse and longitudinal sections, respectively. Villela's etchant revealed a typical tempered martensitic structure in both cases. This type of microstructure was expected since the part was austenitized, quenched, and then tempered.

Close examination of the microstructure at and adjacent to crack regions was conducted to detect any structural changes which may have occurred, as a result of grinding or rubbing during fabrication or in service. There were no areas found that contained unusual precipitation and coagulation of carbides which may have been present if the material had been locally heated to temperatures below A_1.[2] There was also no evidence found of retained austenite. Hardened surfaces containing regions of retained austenite are very sensitive to grinding operations. Sufficient heat or stress caused by heavy grinding can induce transformation of retained austenite to untempered martensite.[3] There were no signs of this type of grain refinement discovered.

There was, however, one unusual feature observed while examining the microstructure of one diaphragm. Another type of structure was discovered outside the fracture region of one longitudinal section as illustrated in Figure 8. This structure was much coarser in appearance than the predominate tempered martensite and contained large white facets, as shown in Figure 9. The structure was located approximately 5/16" away from the edge of the inside diameter and was approximately 1/4" long and 1/16" wide. The region where the structure existed did not experience any cracking and was not in close proximity to any cracks. Microhardness measurements were taken within this area and are listed adjacent to Figure 8. The readings obtained did not differ from those measured of the surrounding microstructure listed in Table 3. An energy dispersive spectroscopy (EDS) analysis was performed within regions of the "coarser" micorstructure to determine if it may have been formed as a result of a nonhomogeneous material. The test did not reveal any foreign elements or impurities. The structure could be a high temperature transformation product. There was no evidence found during this investigation that could relate the formation of the "coarser" microstructure to the cause of cracking.

HARDNESS MEASUREMENTS

An attempt was made to determine if the hardness of the material (SAE 1074 steel) was affected by localized frictional heating during the grinding operation. Grinding burns could cause a lightly tempered condition. Heavy grinding could raise the temperature of localized surface areas into the austenitizing region (1400°F to 1600°F) and then subsequent rapid quenching by the grinding coolant may result in brittle surface layers of untempered martensite. In both cases, these conditions could create regions where the mechanical properties, as well as the microstructure, differ from the interior of the part.

2. RIEDERER-VERLAG. *Grinding Cracks.* ASM Source Book in Failure Analysis, 1974, p. 229.
3. *Ductile and Brittle Fractures.* ASM Metals Handbook, Failure Analysis and Prevention, v. 11, 9th Ed., 1986, p. 89-90.

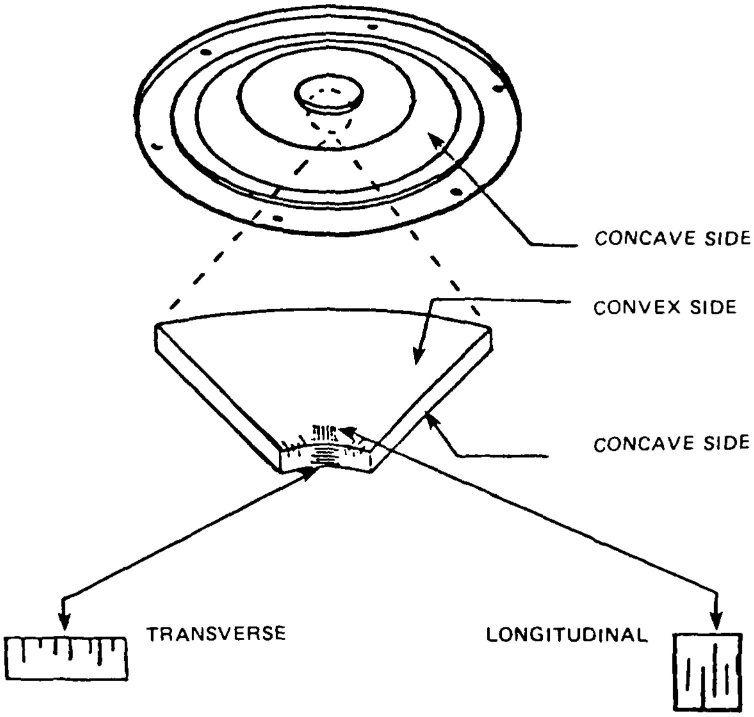

Figure 5. Metallographic sectioning.

Figure 6. Transverse section, Mag. 500X.

Figure 7. Longitudinal section, Mag. 500X.

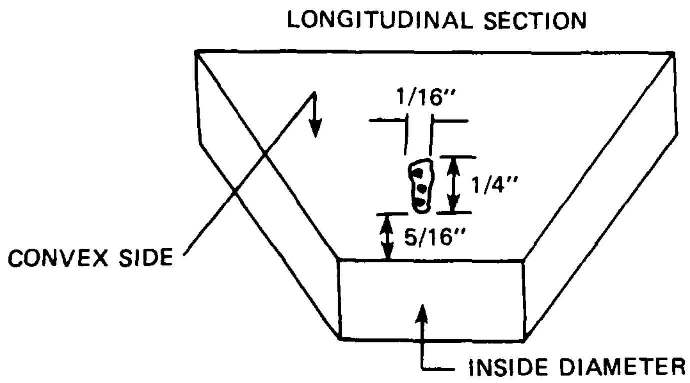

HARDNESS VALUES

Coarse Structure

Knoop	HRC
490	47
487	47
495	47

Figure 8. Illustrates the approximate location of the unusually etched area.

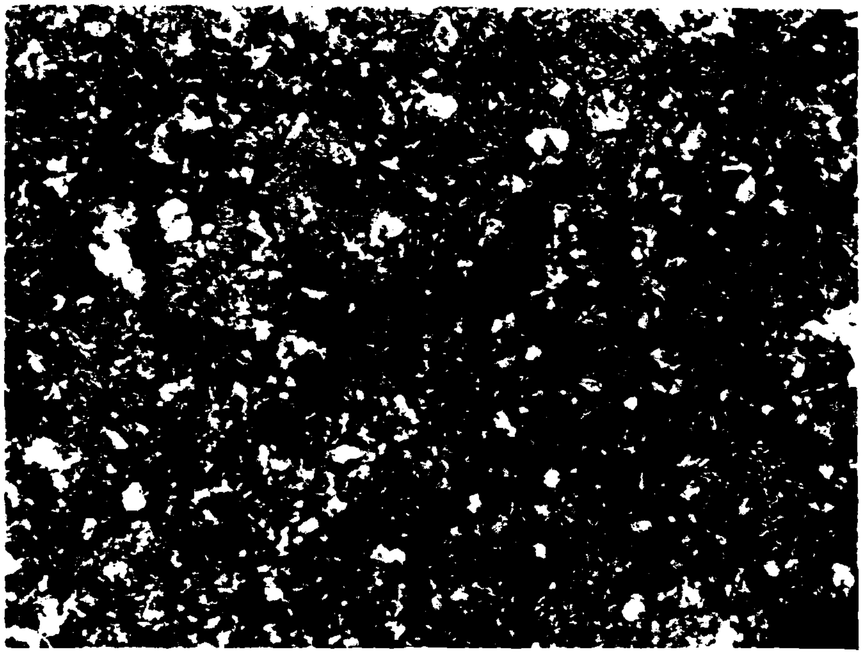

Figure 9. Longitudinal section showing the "Coarser" microstructure surrounded by a martensitic matrix, Mag. 500X.

Microhardness measurements were taken of transverse and longitudinal sections of the inside diameter region. Table 3 schematically points out areas that were tested on two representative samples and also lists the results of these measurements. The Knoop hardness values were converted to Rockwell C scale readings for convenience in comparison. The hardness values that were measured compared favorably with the required hardness range of HRC 42 to 50. The results of this test showed no considerable variation of hardness in a longitudinal or a transverse direction.

Macrohardness measurements were also taken of the diaphragm in an as-received condition. Table 4 illustrates the areas on the convex and concave side of the part that were tested and lists the values of microhardness and macrohardness on the diaphragm. These tests did not reveal any regions which displayed relatively higher or lower degrees of hardness.

VISUAL EXAMINATION

The typical orientation and arrangement of the cracks under investigation can be observed in Figure 10 which is a longitudinal section of the inside diameter. The cracks, as mentioned previously, were located only on the convex side of the diaphragm. In Figure 10, two large cracks can be seen extending radially outward from the edge of the inside diameter. A short distance away, located in the center of the same macrograph, smaller cracks were also formed. All of the cracks observed did not appear to extend more than a quarter of an inch away from the edge of the inside diameter and the depth of the cracks never exceeded the thickness of the diaphragm (0.0895 inch).

Close examination of all the diaphragms investigated, revealed that in every case cracking originated and was confined within a specific region. Figure 11 shows a section taken from a representative diaphragm that contains this area of concern. It was concluded that the region was formed by the lockup clutch piston retaining ring (see Figure 1, Item 12) which caused some mechanical wear on the surface of the diaphragm, where it was located. Abrasion had occurred at contact areas under load between the retaining ring and the diaphragm which were subject to vibration and slip while in service. The area is easily recognized by its shiny, reflective appearance. It can be described as a bright ring which completely circumvents the entire inside diameter. The surface of the ring-like feature is blemished with small indentations and grooves which are the results of the wear previously described. These worn areas on the diaphragm acted as localized stress raisers.[4] Further investigation later revealed that these stress raisers may have been involved with the mechanism that caused the cracking.

SCANNING ELECTRON MICROSCOPY/ENERGY DISPERSIVE SPECTROSCOPY

The cracks were examined under high magnification in order to identify any unusual features of the material or the fracture. Crack branching was observed in many instances. Figures 12 and 13 are as-polished longitudinal and transverse sections, respectively, which show examples of branching. In Figure 13 there appears to be evidence of some type of scale or oxide that has formed on the

4. FONTANA, M. G. *Fretting Corrosion.* Corrosion Engineering, 1986, p. 105-106.

Table 3. DIAPHRAGM - LOCKUP CLUTCH PISTON MICROHARDNESS MEASUREMENTS

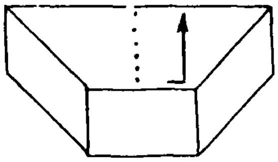

Longitudinal Section

Knoop Hardness
20X - 500 g Load
Diamond Penetrator

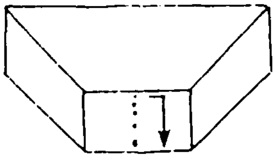

Transverse Section

Distance from Edge of I.D. (mils)	Knoop	HRC	Distance from Edge of I.D. (mils)	Knoop	HRC
-	540	50	-	500	48
4	531	50	4	495	47
9	523	49	9	507	48
14	527	49	14	507	48
22	527	49	24	532	50
32	529	49			
Average:	530	50	Average:	508	48

Table 4. DIAPHRAGM - LOCKUP CLUTCH PISTON MACROHARDNESS MEASUREMENTS

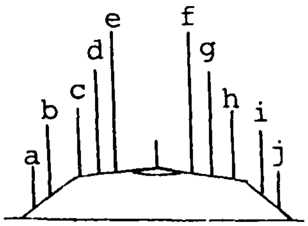

Convex Side

Rockwell Hardness C
Scale 150 Kg Load
Diamond Cone Penetrator

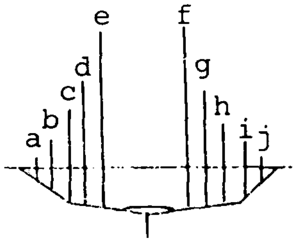

Concave Side

	Distance from Center of I.D. (in.)	HRC		Distance from Center of I.D. (in.)	HRC
a.	3.5	46.5	a.	3.5	46.7
b.	3.0	46.6	b.	3.0	46.7
c.	2.5	46.4	c.	2.5	48.0
d.	2.0	48.4	d.	2.0	49.2
e.	1.5	48.1	e.	1.5	48.3
f.	1.5	48.8	f.	1.5	47.3
g.	2.0	47.5	g.	2.0	47.5
h.	2.5	48.9	h.	2.5	47.9
i.	3.0	47.0	i.	3.0	46.9
j.	3.5	46.8	j.	3.5	47.4
	Average:	47.5		Average:	47.6

Figure 10. Longitudinal section showing a cracked region of the inside diameter. Arrows indicate the area formerly occupied by the retaining ring, Mag. 30X.

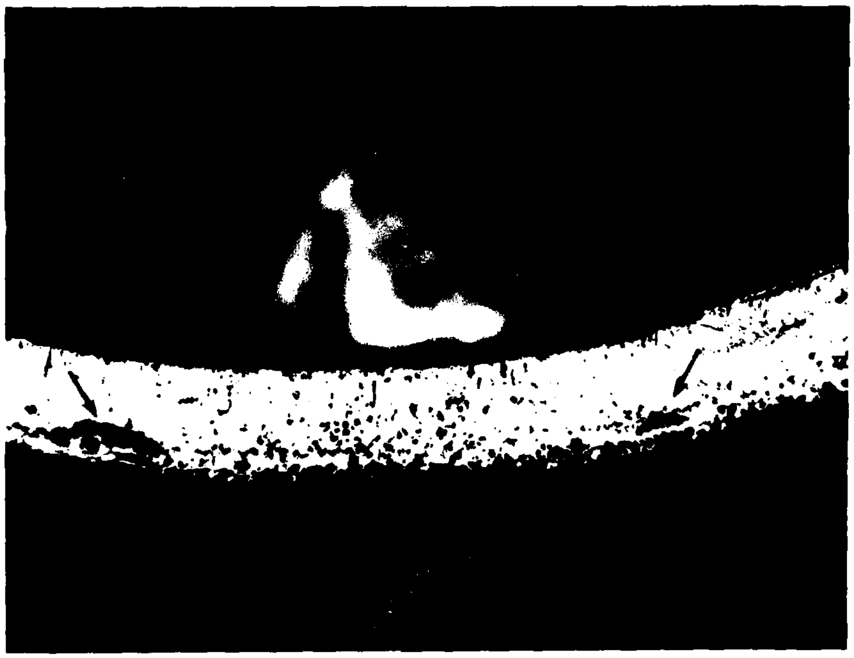

Figure 11. Longitudinal section identifying the contact area between the retaining ring and the diaphragm. The arrows point out shallow grooves cut into the surface. Note the abrasion that has occurred, Mag. 7.5X.

fracture surface. This was later confirmed by energy dispersive spectroscopy (EDS) when the fracture surface was investigated. Figure 14 shows the spectra obtained from the EDS analysis performed on one typical area from the fracture (see Figure 13 for exact location). As expected, it contained mainly Fe and O, and very small amounts of Al and Si. The Al could be the result of polishing or the base material may have been Al killed during primary processing.

While examining the surfaces of cracked regions, it was found that cracking was sometimes associated with inclusions and other discontinuities in the material. Figure 15 reveals such an instance. Here a crack has originated at the surface irregularity. This small defect acted as a stress concentration area and when the stress parameters of the material were exceeded, a crack initiated here. Figure 16 shows the presence of inclusions over the entire surface of a longitudinal section. In many areas, cracks were found propagating through inclusions and in other instances cracks had originated at sites occupied by inclusions. Some of these were identified as manganese sulfide inclusions. Figure 17 illustrates representative results obtained from an EDS analysis performed on three different regions (see Figure 16 for exact locations).

The typical spectra from these regions show large amounts of Fe, S, and Mn. Transverse fracture toughness and ductility can be decreased by these inclusions. Fatigue crack propagation characteristics of the material and corrosion resistance are also adversely effected.[5] It was concluded that although these inclusions may have contributed in some instances to the cracking observed, they are not the primary cause, since many of the cracks examined were not associated to any extent with these inclusions and the material itself was not considered a "dirty steel."

The fracture surfaces of a series or cracks were examined by utilizing the following procedure:

- Small sections containing cracks were cut from the diaphragm
- The samples were then placed in liquid nitrogen and cooled to a very low temperature
- The specimens were then quickly placed in a vise and one half of the fracture surface was bent away from the other by striking it with a hammer.

Figure 18 is a SEM fractograph showing the general appearance of one fracture surface. The "thumbnail" crack shown here was indicative of many of the cracks examined. The shape of this type of fracture usually suggests a single point crack origin which may occur as a result of an inclusion or notch. Further examination was conducted later in the investigation to determine the crack initiation site. The crack was outlined by a dark corrosion product. Outside the crack fast fracture occurred when the specimen was struck by the hammer during the opening procedure. Laminated structures, which were found to be the result of prior fabrication procedures, can be seen running horizontally across the fracture surface. Most of these structures were identified as groups of prior austenitic grains which had become elongated as a result of cold working, while a few were found to be elongated manganese sulfide inclusions through EDS analysis.

5. JOSEPH, R. A., and TIPNIS, V. A. *The Influence of Non-Metallic Inclusions on the Machinability of Free-Machining Steels.* ASM Materials/Metalworking Technology Series, no. 7, 1975.

Higher magnification of the same crack as seen in Figure 19 reveals a surface film and debris. An attempt was made at this point to determine the fracture mode and the crack origin. In order to accomplish this, it was necessary to clean the specimen because it was unsuitable for further conclusive fractographic observations. The cleaning process involved ultrasonic cleaning of the sample in a detergent solution which was then followed by electrochemical cleaning in an Endox 214 solution.[6] This technique does not damage the base metal.

Figure 20 shows the same fracture surface at the same magnification as Figure 19 after cleaning was performed. The fracture mode was identified as being quasi-cleavage. There were no intergranular features found. The crack origin can be seen at the center of the crack near the top edge of the micrograph. There were no inclusions or other unusual features associated with the crack origin. There was also no evidence of fatigue striations or rub marks which are striation-like linear indications produced by rubbing or abrasion.

The crack origin was examined at 1500X as shown in Figure 21, confirming that the fracture mode was indeed quasi-cleavage. Again, there was no indication of any irregularities such as an inclusion or a notch at the crack initiation site. A quasi-cleavage mode of fracture as apposed to an intergranular mode of fracture strongly indicated that these cracks were not associated with the quenching or grinding operations. Quench cracks are generally characterized as being intergranular.[7] Grinding cracks are also intergranular in nature.[8]

Further investigation of various cracks revealed another important feature which was associated with a small number of fracture surfaces examined. Figure 22 is a representative example of one such fracture surface that contains this feature. The arrow at the bottom of this SEM fractograph points out the origin of the crack and located just above this site are macroscopic progression marks on the fracture surface. These markings were concluded to indicate successive positions of the advancing crack front and were probably formed as a result of a change in loading during crack propagation.

Figure 23 shows the same fracture surface under lower magnification 15X in order to point out the difference in appearance between the surface film observed on this fracture surface and the one shown in Figures 18 and 19. The film covering the original fracture in Figure 23 is much less pronounced (and is barely visible), whereas the film shown in Figures 18 and 19 is thicker, darker, and is easily distinguished. If these cracks were the result of the quenching operation, a high temperature, tempering oxide would have been expected to form on all exposed fracture surfaces as a result of the subsequent tempering operation. The exact type of oxide film that had formed on the walls of the cracks could not be determined. The film was too thin in all instances to examine by X-ray diffraction techniques.

The fracture surfaces of the cracks were examined by EDS. Figure 24 is an example of one fracture showing the areas which were investigated. Figure 25 shows representative results of the spectra obtained in areas 1 and 2 near the crack origin. Large amounts of Fe were detected, along with a trace of Si. There were no

6. YUZAWICH, P. M., and HUGES, C. W. *An Improved Technique for Removal of Oxide Scale from Fractured Surfaces of Ferrous Materials.* Practical Metallography, 1979, p. 184-194.
7. *Fatigue Failures.* ASM Metals Handbook, Failure Analysis and Prevention, v. 11, 9th Ed., 1986, p. 122.
8. PHILLIPS, A., and KERLINS, V. *Analyzing Fracture Characteristics by Electron Microscopy.* ASM Source Book in Failure Analysis, 1974, p. 394.

foreign elements, such as Cl present. The SEM fractograph of this area reveals the presence of a scale and debris. Figure 26 shows the spectra of area 3. The only difference discovered is the addition of a small amount of Mn. The laminated structures are quite visible in the SEM fractograph taken of this area. The fracture morphology in area 3 is clearly distinct because of the absence of a thick film or corrosion products.

MECHANICS ANALYSIS

Methods

It is the practice of mechanical designers to include stress-concentration factors when designing parts having geometries which increase the local stress intensity. Design features such as holes, fillets, sharp edges, and grooves are included in tables which list their magnification of stress. A crack will also act as a stress concentrator. The degree of intensity at the crack tip is a function of the geometry of the part, the type of loading, the length of the crack, and the radius of the crack tip. The intent of this section is to determine the following:

1. Calculate the actual operating stress in the diaphragm.
2. Measure the residual stresses near the edge of the inside diameter by the use of X-ray diffraction.
3. Calculate the critical stress-intensity factor (K_{IC}) for the material (SAE 1074 steel quench and tempered).
4. Calculate the stress-intensity factor (K_I) for the conditions observed.
5. Calculate the possible crack propagation rates under actual loading conditions.

Section 1

The maximum operating stress in the diaphragm was determined by using the thin-walled pressure vessel theory, where t = Pr/2t.[9] First the radius of curvature of the diaphragm was calculated as shown below:

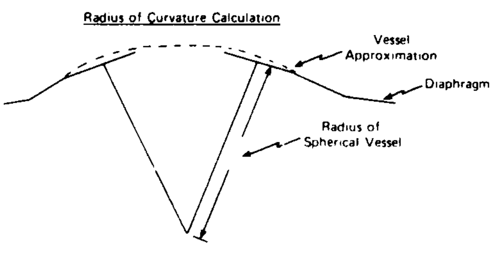

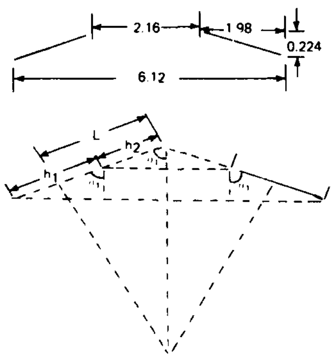

$$\sigma_1 = \text{ARCTAN } \frac{1.977}{0.224} = 83.5°$$

$$L = \frac{h_1}{2} + h_2$$

$$h_1 = \sqrt{(1.98)^2 + (0.224)^2} = 1.99''$$

$$h_2 = \frac{2.16}{2} \;/\; \text{SIN } \sigma_1 = 1.09''$$

$$L = \frac{1.99}{2} + 1.09 = 2.05''$$

$$r = L \text{ TAN } \sigma_1 = 18.3''$$

9. BEER, F. P., and JOHNSTON, F. R. *Mechanics of Materials.* McGraw-Hill Inc., NY, 1981, p. 325-327.

The operating stress was calculated to be 18.4 ksi.

σ_t = stress

P = pressure (oil) 180 psi

r = radius 18.3

t = thickness 0.895

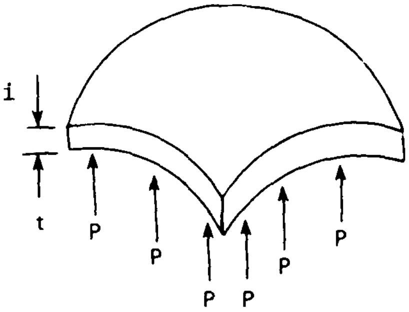

FOR A THIN VESSEL ⟶ $t \leqslant 1/20r$

$t = 0.895"$

$1/20r = 1.35$

$$\sigma_t = \frac{Pr}{2t} = \frac{(180)\ (18.3)}{2(0.0895)}$$

σ_t = 18.4 ksi

Section 2

The results of the residual stress measurements on one representative diaphragm are listed in Table 5. These values are accurate within a range of ± 0.5 ksi.

Table 5. RESIDUAL STRESS MEASUREMENTS ON A DIAPHRAGM

Convex Side		Concave Side	
Distance from Edge of I.D. (mm)	Residual Stress (ksi)	Distance from Edge of I.D. (mm)	Residual Stress (ksi)
2	4.5 tensile	2	42.7 compressive
4	46.4 tensile	4	49.0 compressive
6	42.7 tensile	6	44.5 compressive
8	63.6 tensile	8	30.9 compressive
10	41.8 tensile	10	30.0 compressive

Section 3

Rolfe and Barson present a Charpy V-notch (CVN) conversion to K_{IC} in, "Fracture and Fatigue Control in Structures," where $K_{IC}^2/E = A$ (CVN). This equation is an approximation of the K_{IC} and is based on the fact that the CVN impact energy absorption curve for constructional steels undergoes a transition in the same temperature zone as the impact plane-strain fracture toughness.[10] The CVN values for 1075 - hardened steel at 0°F and 80°F were 12 ft-lb and 15 ft-lb, respectively.[11] The equation yielded the following results:

K_{IC} = critical plane-strain stress intensity factor (ksi$\sqrt{\text{in.}}$)

CVN = Charpy V-notch value (15 ft-lb, 12 ft-lb)

E = modulus of elasticity (30 x 10^6 psi)

A = constant of proportionality (4)

10. ROLFE, S. T., and BARSON, J. M. *Fracture and Fatigue Control in Structures.* Prentice-Hall, Englewood Cliffs, NJ, 1977, p. 180.
11. *High Carbon Steel.* MPDC Battelle, Structural Alloys Handbook, v. 1, 1986, p. 10.

for CVN = 15 ft-lb	for CVN = 12 ft-lb
$K_{IC}^2 = A\ (CVN)\ E$	$K_{IC}^2 = A\ (CVN)\ E$
$K_{IC} = 42.4\ ksi\sqrt{in.}$	$K_{IC} = 38.0\ ksi\sqrt{in.}$

Section 4

The Irwin Analysis for quarter ellipitical cracks at a hole was used to calculate the K_I value under actual loading conditions and at measured crack parameters. The crack depths and lengths were measured at 200X using a recticle and a stage micrometer. A representative listing of data is shown in Table 6. The sample that was used contained 28 cracks within a length of 0.625 inch. The measurements were taken before the cracks were opened for fractographic examination.

Table 6. CRACK MEASUREMENTS

Crack I.D. No.	Depth (in.)	Length (in.)
1	0.0035	0.1700
2	0.0012	0.0610
3	0.0012	0.0350
4	0.0077	0.0500
5	0.0032	0.2170
6	0.0012	0.2300
7	0.0009	0.0150
8	0.0029	0.1880
9	0.0093	0.2150
10	0.0032	0.1740
11	0.0039	0.1630
12	0.0014	0.0610
13	0.0007	0.0940
14	0.0024	0.1980
15	0.0059	0.2090
16	0.0054	0.2070
17	0.0034	0.1000
18	0.0029	0.0970
19	0.0046	0.1260
20	0.0104	0.1560
21	0.0034	0.2030
22	0.0034	0.2150
23	0.0025	0.1900
24	0.0340	0.1700
25	0.0207	0.2450
26	0.0059	0.0320
27	0.0440	0.0400
28	0.0018	0.0910

The K_I values were determined by using the equation:

$$K_I = \frac{1.2\sqrt{P}}{\phi} \quad 1 + \frac{P^2\ (D-q)^2}{4D^2q^2} \quad 1/4 \qquad \text{(Ref. 12)}$$

where K_I = Stress Intensity Factor
p = Crack Depth
q = Crack Length
D = Hole Diameter
ϕ = Elliptical Integral
σ = Stress in Material.

The hole diameter "D" was measured to be 2.165 inches. Various crack parameters were used in calculating the K_I value. The values for "P" and "q" were determined from various measurements taken from Table 6. The stress in the material "σ" was determined by adding the highest value of residual stress listed in Table 5 to the actual operating stress calculated in Section 1. The flaw shape parameter can be derived from the figure shown below:

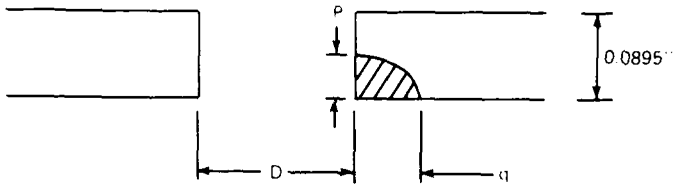

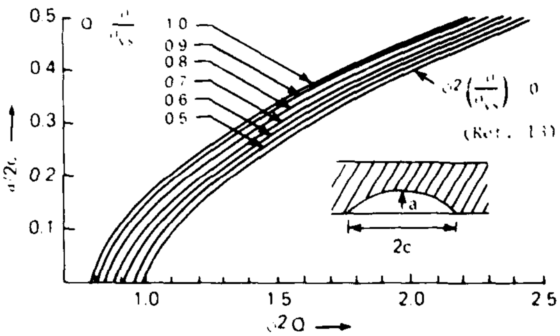

Surface flaw parameter

For a crack where $P = 0.04$ $\qquad K_I = 33.4$ ksi$\sqrt{\text{in}}$.
$q = 0.04$
$\sigma = 18.4 + 63.6 = 82$ ksi

Example II

For a crack where $P = 0.02$ $\qquad K_I = 16.0$ ksi$\sqrt{\text{in}}$.
$q = 0.16$
$\sigma = 18.4 + 63.6 = 82$ ksi

Example III

For a crack where $P = 0.01$ $\qquad K_I = 16.0$ ksi$\sqrt{\text{in}}$.
$q = 0.16$
$\sigma = 18.4 + 63.6 = 82$ ksi

12. BROEK, D. *Martinus Elementary Engineering Fracture Mechanics*, Alphen aan den Rijn: Sijthoff and Noordhoff, 1982, p. 354.
13. BROEK, D. *Martinus Elementary Engineering Fracture Mechanics*, Alphen aan den Rijn: Sijthoff and Noordhoff, 1982, p. 82.

Section 5

The final section of the mechanics analysis is devoted to calculating the possible fatigue crack propagation rates under loading conditions.

For martensitic steels, where y ≥ 80 ksi

(Crack Propagation Rate) $\frac{da}{dN} = 0.66 \times 10^{-8} (\Delta K_I)^{2.25}$ (Ref. 14).

The ΔK values which are used are typical for the loading conditions encountered

$$\text{at } \Delta K_I = 7, \quad \frac{da}{dN} = 0.66 \times 10^{-8} (7.0)^{2.25} = 5 \times 10^{-7} \text{ inch/cycle}$$

$$\text{at } \Delta K_I = 10, \quad \frac{da}{dN} = 0.66 \times 10^{-8} (10)^{2.25} = 1.2 \times 10^{-6} \text{ inch/cycle.}$$

RESULTS OF THE MECHANICS ANALYSIS

The calculated maximum operating stresses in the diaphragm were relatively low but the surface residual tensile stresses within the fractured region were considerably high. This facet lead to the conclusion that the residual stresses were the leading contributor to the cracking of the inside diameter. In some instances, as demonstrated in Section 4, the K_I values that were calculated approached the K_{IC} values for the material. If the operating stresses were to increase due to improper or abusive clutch engagement then there would be examples of the K_I value approximating the K_{IC} value. In these cases, there is a risk of rapid crack propagation. The calculation of the crack propagation rates indicate that at $\Delta K_I = 7$ the rate is slow, but at $\Delta K_I = 10$ the rate is moderate. Both values of ΔK_I are typical for the type of loading conditions encountered. Such factors as distribution of stress within the part, corrosion, and the number of cycles encountered will effect the useful service life of the diaphragm. Plane-strain conditions have been assumed when calculating the values in the mechanics analysis. These figures are approximations and have been utilized within the context of this examination as such.

DISCUSSION

The type of steel used to fabricate the diaphragm (SAE 1074) contains a large amount of carbon which increases hardness and strength but also lowers ductility making it more difficult to form and machine. The laminated structure of the material indicated prior material processing. The deformation procedures used to cut the part, to shape it, and to pierce out its inside diameter were all performed at room temperature. These fabrication processes all contributed toward increasing the residual stresses in the material, especially near the inside diameter region, which was blanked, and the highest residual stresses were measured. The diaphragm contained considerably high residual tensile stresses on the convex surface near the inside diameter. This area was where cracking occurred. When the measured residual stresses were added to the operating stresses, the combined total approximated

14. ROLFE, S. T., and BARSON, J. M. *Fracture and Fatigue Control in Structures.* Prentice-Hall, Englewood Cliffs, NJ, 1977, p. 236.

50 percent of the yield strength of the material, in some instances. The residual stress measurements were taken after cracking had occurred and the material was in a more relaxed condition. This suggests that the residual stresses in the material prior to cracking would have been much higher.

Local surface imperfections, such as scratches, marks, or grooves which were the result of mechanical abrasion caused by the lockup clutch piston retaining ring are the most likely sites where cracks may have nucleated when the stress parameters of the material were exceeded. Examples of this were found as previously explained (refer to Figure 15). These areas acted as stress concentrators magnifying an already high internal stress, caused by prior fabrication processes.

The fracture morphology of all the cracks examined was quasi-cleavage, which indicated that cracking was not due to quenching or grinding because these operations would have caused an intergranular mode of fracture. There was also no indication of grain refinement or any differences in hardness measured within the area of concern, both of which may be caused by excessive grinding. The grinding and the quenching operations would have also contributed toward increasing internal stresses within the material. However, if a proper tempering treatment was performed immediately after quenching, damaging internal stresses would have been relieved. If care was excerised during the grinding operation, tensile stresses, which might have formed as a result of this operation, would have been offset by the compressive stresses introduced into the material during subsequent shot peening.

The fracture faces of the cracks observed were entirely covered with an oxide film and debris. The type of oxide film that formed on the walls of the cracks could not be determined. The film was too thin to examine by X-ray diffraction techniques. Distinguishing between a high temperature oxide film and one that formed in an air environment at lower temperatures would help to determine at what point in the life of the part that cracking occurred. Another approach to this problem would have been to perform in-process inspections of the part at each of the various manufacturing operations to discover if cracking occurred during any of these operations. This, however, was impossible since the diaphragm is currently produced by a different manufacturer, made from a different type of steel (SAE 6150) and the cracking problem no longer exists. Knowing if the part had cracked during manufacturing would have also ruled out or possibly confirmed that cracking may have been caused by fatigue.

This investigation did not reveal any conclusive evidence that would support fatigue as the sole mechanism of failure. An attempt was made to examine newly manufactured parts that had not been placed in service. This was not possible since the particular diaphragms under investigation had not been produced since 1980 to 1981, and all of those that were produced prior to this time had all been in service. Fatigue cracks may be transgranular of intergranular in nature but the most prominent features found are the existence of fatigue striations. These features were not found on any of the parts examined. In steels, fatigue striations may not be always well defined under ordinary crack-growth rates and are often difficult to distinguish, especially if the fracture surface is covered with an oxide or corrosion products.[15] These factors must be considered and the possibility of fatigue assisted cracking cannot be entirely ruled out.

15. *Fatigue Failures.* ASM Metals Handbook, Failure Analysis and Prevention, v. 11, 9th Ed., 1986, p. 105.

High strength, tempered steels with hardness values of HRC 46 and above are extremely susceptible to cracking due to hydrogen embrittlement (HE) and also stress corrosion cracking (SCC). However, the part was not located in an environment conducive to these mechanisms of failure and there was no evidence to support the presence of an embrittling agent. In the case of (SCC) there are generally some corrodants, such as Cl, Na, or S found trapped in the corrosion products on the fracture surfaces, but none were discovered. These mechanisms were probably not involved in the cracking of the part.

CONCLUSIONS

The main purpose of this investigation was to determine if a diaphragm that contained cracks near the inside diameter region could be placed back into service without any risk of subsequent failure. Conjunctively, the probable causes for these cracks were also investigated. This metallurgical evaluation had led to the following conclusions.

1. TACOM reference P/N 6769139 Diaphragm Lockup Clutch Piston, should not be placed back into service if there is any evidence of circumferential cracks originating and extending radially from the inside diameter.

   - Residual stress measurements taken of the surface, after cracking had occurred, revealed considerably high tensile stresses within the area of concern. There is a risk of further crack propagation because these stresses in combination with the actual operating stresses are intensified at the crack tip of existing fractures. If this part should fail in service, proper clutch application would be adversely effected due to a loss in oil pressure making gear engagement difficult or impossible to achieve.

2. The cracking experienced by the diaphragm was not determined to be primarily service related. However, a complete evaluation of the part's life cycle could not be accomplished making it difficult to conclude an exact mechanism of failure. The following, important, pieces of information would have allowed for a more complete and conclusive examination:

   - In-process inspection of the manufacturing operations
   - Analyses of parts that had not been placed in service
   - A determination of the type of surface film/films that had formed on the walls of the fractured surfaces

   Cracking was probably not caused by the following:

   - Grinding cracks
   - Quench cracks
   - Stress corrosion cracking
   - Hydrogen embrittlement

   If cracking did not occur during manufacturing, it may have occurred while the part was actually in service. As previously explained cracking originated and was confined within an area formerly occupied by the lockup clutch piston retaining ring. Cracks could have resulted from the abrasive action of this retaining ring on the surface of the diaphragm.

- High internal stresses within the material that were the result of prior material processing, coupled with the actual operating stresses were concentrated and intensified at small nicks, grooves, and scratches caused by the mechanical wear of the retaining ring. Eventually, as this abrasive action continued and these surface defects deepened, the stress parameters of the material were exceeded causing cracks to initiate from these areas. The cracks most likely propagated rapidly until a sufficient amount of stress was alleviated from the material and the crack front reached an area of lower internal stress.

- During the period that cracking took place, changes in loading (i.e., clutch engagement/disengagement) could have caused progression marks to form on some of the fracture surfaces. The surface films which had formed on the walls of the cracks were more pronounced and thicker on some cracks than on others. The varying condition of these surface films may have been attributed to any or all of the following:

  - The cracks may not have all formed at the same time.

  - The part had been in storage and then placed back into service for undetermined lengths of time. This allowed the cracks to have varying exposure times under storage conditions and service conditions.

  - The operating temperatures of the diaphragm have exceeded 300°F. This would also cause the cracks to be exposed to different environments for varied periods of time.

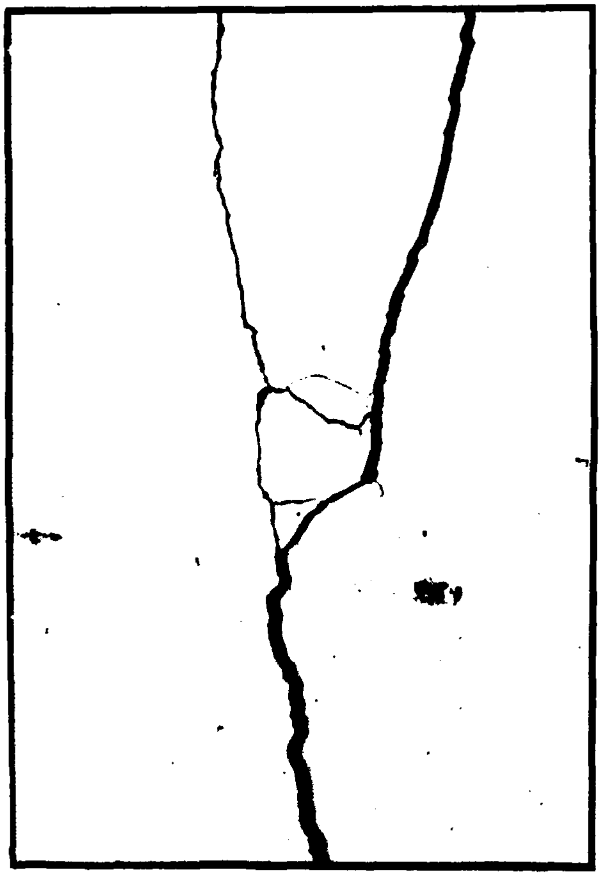

Figure 12. Longitudinal section showing an example of crack branching, Mag. 500X.

Figure 13. Transverse section revealing the presence of a surface film on the fracture surface, Mag. 1000X.

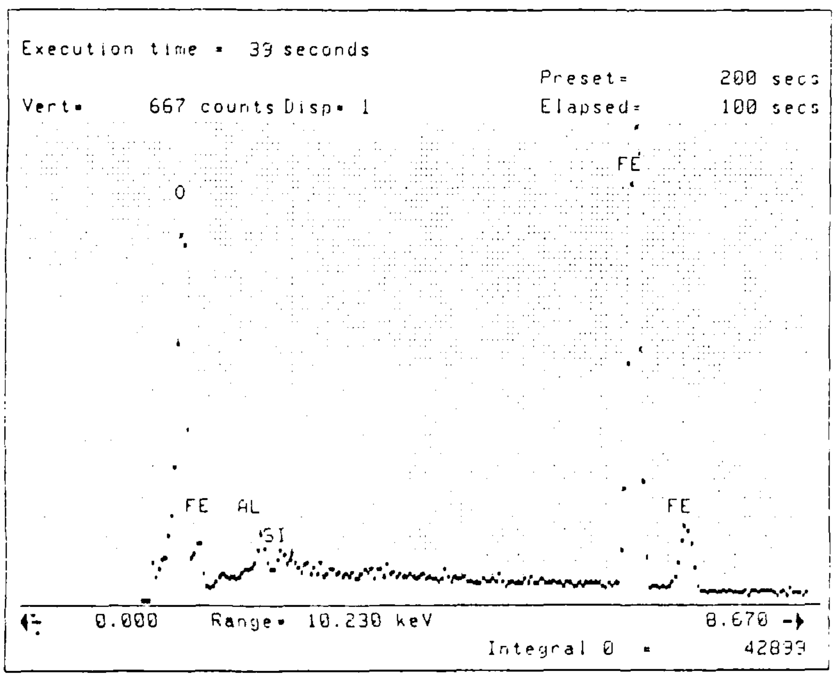

Figure 14. EDS spectra of the area identified in Figure 13.

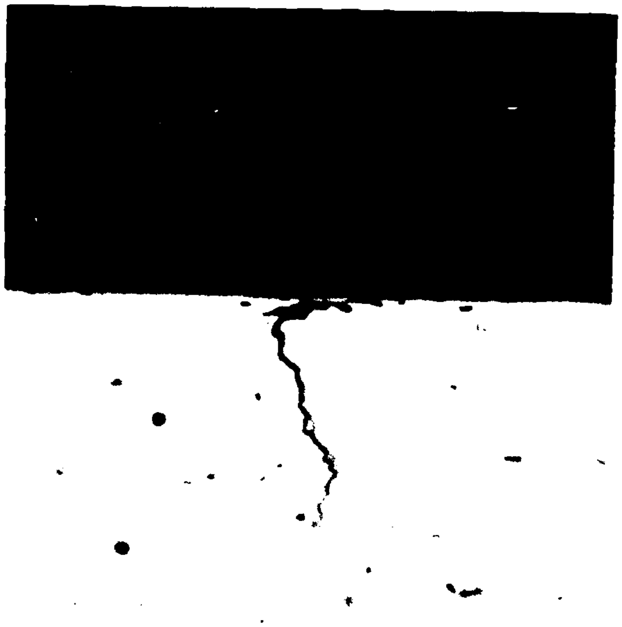

Figure 15. Transverse section showing a crack that initiated at a surface irregularity, Mag. 1000X.

Figure 16. Longitudinal section reveals inclusions within the material, Mag. 500X.

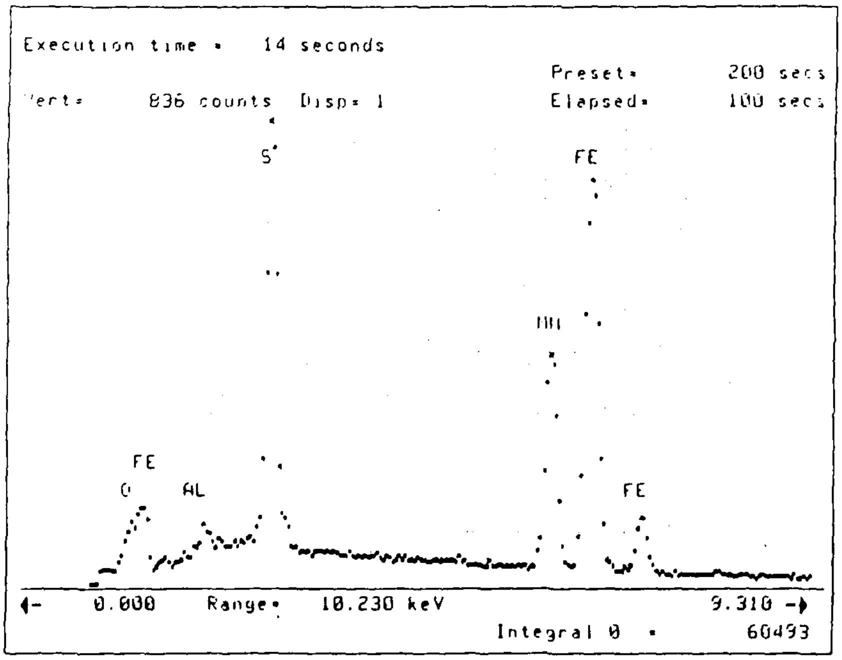

Figure 17. Typical EDS spectra of the areas identified in Figure 16.

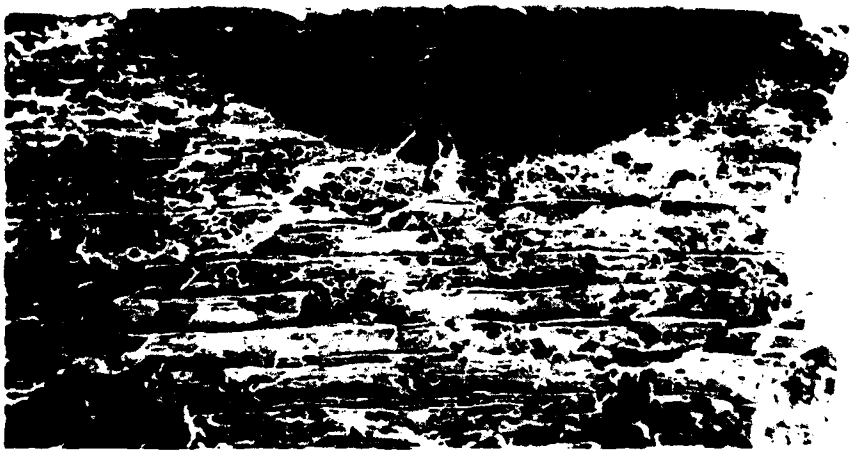

Figure 18. Fractograph showing the general appearance indicitive of many of the cracks examined, Mag. 80X.

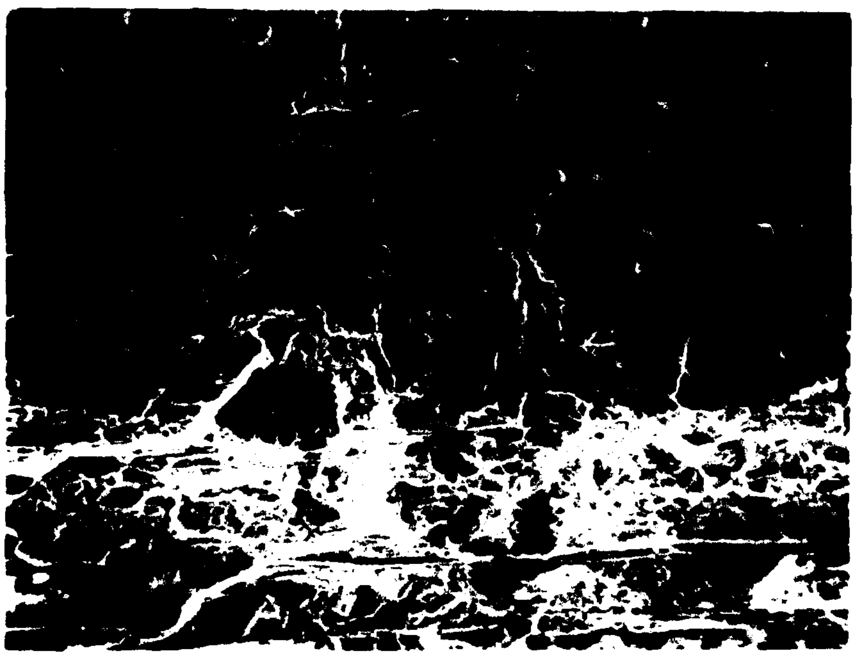

Figure 19. Fractograph revealing a surface film and debris on the fracture, Mag. 250X.

Figure 20. Fractograph identical to Figure 19, but after cleaning was performed. The crack origin can be seen near the top edge of the fractograph, Mag. 250X.

Figure 21. Fractograph confirming a quasi-cleavage fracture mode and the absence of any unusual features associated with the crack origin, Mag. 1500X.

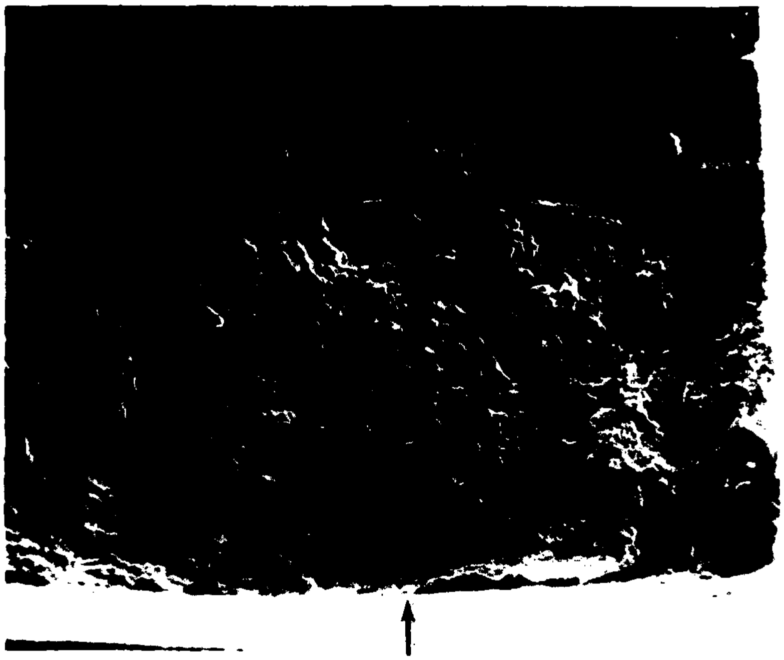

Figure 22. Fractograph revealing the crack origin and progression marks near the bottom edge, as indicated, Mag. 80X.

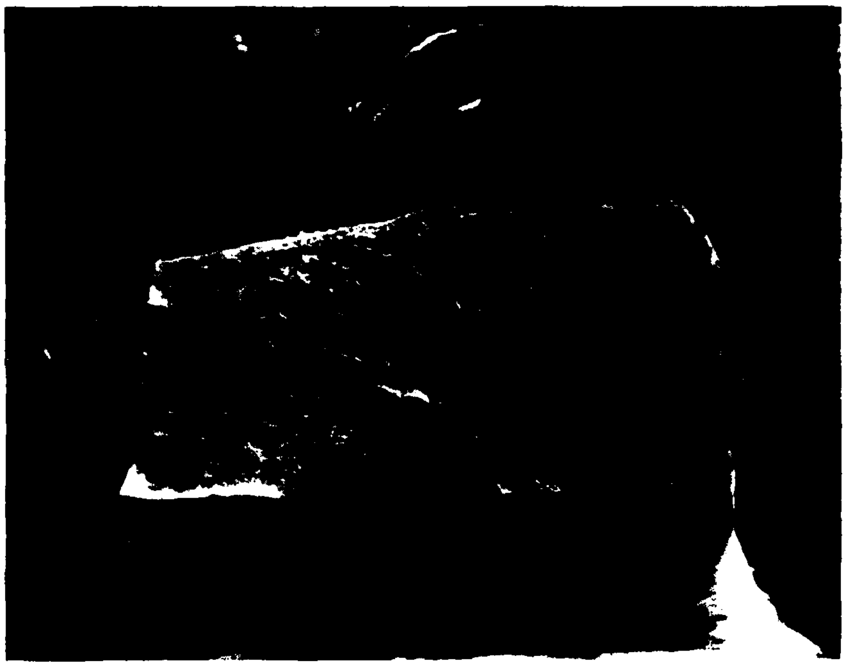

Figure 23. Fractograph showing a less pronounced surface film, Mag. 15X.

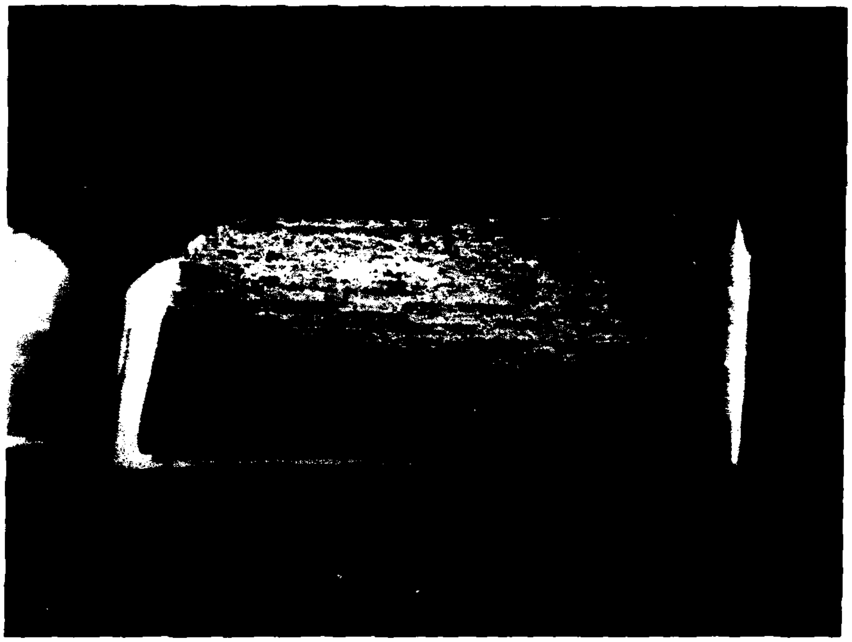

Figure 24. Fractograph showing areas that were examined by EDS, Mag. 15X.

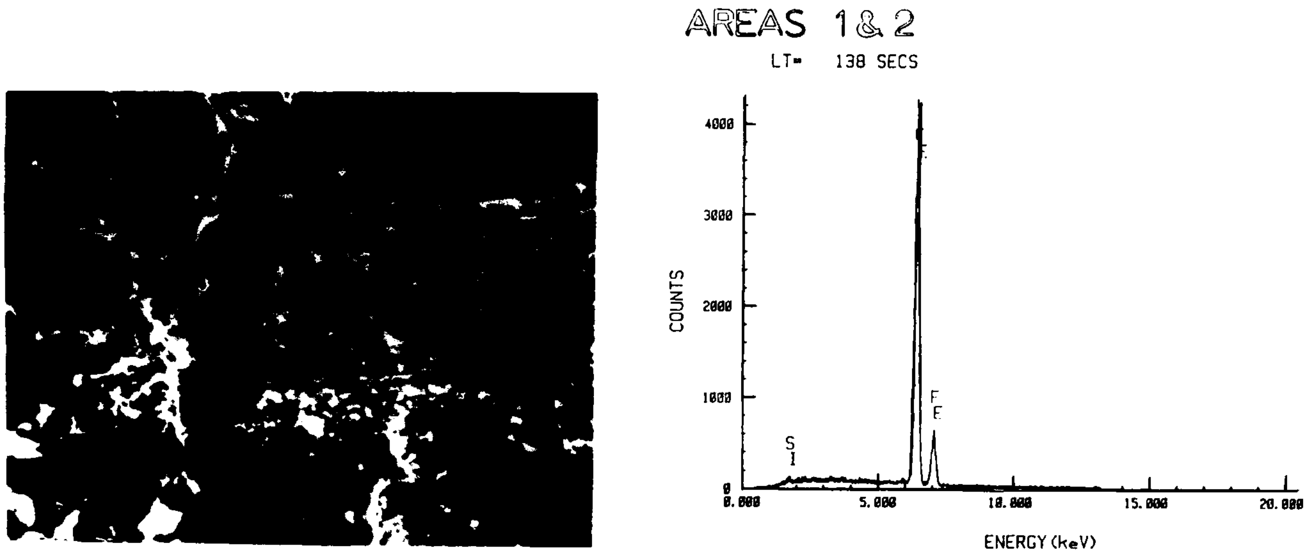

Figure 25. Fractograph and corresponding EDS spectra representative of areas 1 and 2 of Figure 24, Mag. 500X.

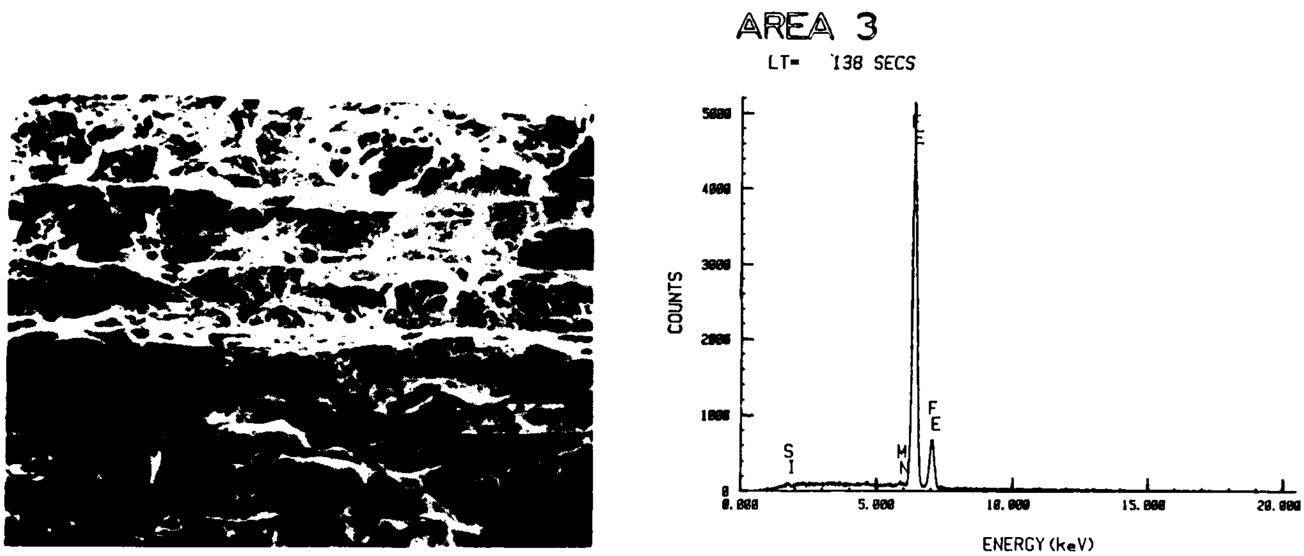

Figure 26. Fractograph and corresponding EDS spectra representative of area 3 on Figure 24, Mag. 500X.

ACKNOWLEDGMENT

The request for this metallurgical examination was initiated by Mr. Brian Rich of Anniston Army Depot.

The author wishes to extend thanks to Dr. N. Tsangarakis, Dr. R. Sisson, R. Middleton, and A. Zani for their helpful discussions.

DISTRIBUTION LIST

No. of Copies	To
	Commander, U.S. Army Laboratory Command, 2800 Powder Mill Road, Adelphi, MD 20783-1145
1	ATTN: SLCIS-IM-TL
	Commander, Defense Technical Information Center, Cameron Station, Building 5, 5010 Duke Street, Alexandria, VA 22304-6145
2	ATTN: DTIC-FDAC
	Commander, U.S. Army Materiel Command, 5001 Eisenhower Avenue, Alexandria, VA 22333
1	ATTN: AMCLD
	Anniston Army Depot, Anniston, AL 36201
1	ATTN: Mr. Brian Rich, Mechanical Engineer
	Director, U.S. Army Materials Technology Laboratory, Watertown, MA 02172-0001
2	ATTN: SLCMT-IML
1	Author

U.S. Army Materials Technology Laboratory
Watertown, Massachusetts 02172-0001
METALLURGICAL EXAMINATION OF A DIAPHRAGM - LOCKUP CLUTCH PISTON - Victor K. Champagne, Jr.

Technical Report MTL TR 88-6, April 1988, 33 pp - illus-tables

AD__________

UNCLASSIFIED
UNLIMITED DISTRIBUTION

Key Words

Clutch Piston
High carbon steels
Failure

A metallurgical examination was performed on a diaphragm - lockup clutch piston which experienced cracking around the inside diameter. The study required reviewing the manufacturing procedures, analyzing the service conditions, and determining the operating stresses induced on the part in service. The extent of cracking was verified by using magnetic particle testing. Material identification and characterization was accomplished by performing mechanical testing, chemical analysis, and metallographic techniques. Scanning electron microscopy (SEM) and electron dispersive spectroscopy (EDS) was used to examine features of the material and the fracture surface. Finally, a mechanics analysis was included in order to calculate an approximation of the actual operating stresses, the critical stress-intensity factor (K_{IC}) for the material, the stress-intensity factor (K_I) under observed conditions, and the possible crack propagation rates under actual loading. Measurements of the residual stress were also taken utilizing X-ray diffraction.

U.S. Army Materials Technology Laboratory
Watertown, Massachusetts 02172-0001
METALLURGICAL EXAMINATION OF A DIAPHRAGM - LOCKUP CLUTCH PISTON - Victor K. Champagne, Jr.

Technical Report MTL TR 88-6, April 1988, 33 pp - illus-tables

AD__________

UNCLASSIFIED
UNLIMITED DISTRIBUTION

Key Words

Clutch Piston
High carbon steels
Failure

A metallurgical examination was performed on a diaphragm - lockup clutch piston which experienced cracking around the inside diameter. The study required reviewing the manufacturing procedures, analyzing the service conditions, and determining the operating stresses induced on the part in service. The extent of cracking was verified by using magnetic particle testing. Material identification and characterization was accomplished by performing mechanical testing, chemical analysis, and metallographic techniques. Scanning electron microscopy (SEM) and electron dispersive spectroscopy (EDS) was used to examine features of the material and the fracture surface. Finally, a mechanics analysis was included in order to calculate an approximation of the actual operating stresses, the critical stress-intensity factor (K_{IC}) for the material, the stress-intensity factor (K_I) under observed conditions, and the possible crack propagation rates under actual loading. Measurements of the residual stress were also taken utilizing X-ray diffraction.

U.S. Army Materials Technology Laboratory
Watertown, Massachusetts 02172-0001
METALLURGICAL EXAMINATION OF A DIAPHRAGM - LOCKUP CLUTCH PISTON - Victor K. Champagne, Jr.

Technical Report MTL TR 88-6, April 1988, 33 pp - illus-tables

AD__________

UNCLASSIFIED
UNLIMITED DISTRIBUTION

Key Words

Clutch Piston
High carbon steels
Failure

A metallurgical examination was performed on a diaphragm - lockup clutch piston which experienced cracking around the inside diameter. The study required reviewing the manufacturing procedures, analyzing the service conditions, and determining the operating stresses induced on the part in service. The extent of cracking was verified by using magnetic particle testing. Material identification and characterization was accomplished by performing mechanical testing, chemical analysis, and metallographic techniques. Scanning electron microscopy (SEM) and electron dispersive spectroscopy (EDS) was used to examine features of the material and the fracture surface. Finally, a mechanics analysis was included in order to calculate an approximation of the actual operating stresses, the critical stress-intensity factor (K_{IC}) for the material, the stress-intensity factor (K_I) under observed conditions, and the possible crack propagation rates under actual loading. Measurements of the residual stress were also taken utilizing X-ray diffraction.

U.S. Army Materials Technology Laboratory
Watertown, Massachusetts 02172-0001
METALLURGICAL EXAMINATION OF A DIAPHRAGM - LOCKUP CLUTCH PISTON - Victor K. Champagne, Jr.

Technical Report MTL TR 88-6, April 1988, 33 pp - illus-tables

AD__________

UNCLASSIFIED
UNLIMITED DISTRIBUTION

Key Words

Clutch Piston
High carbon steels
Failure

A metallurgical examination was performed on a diaphragm - lockup clutch piston which experienced cracking around the inside diameter. The study required reviewing the manufacturing procedures, analyzing the service conditions, and determining the operating stresses induced on the part in service. The extent of cracking was verified by using magnetic particle testing. Material identification and characterization was accomplished by performing mechanical testing, chemical analysis, and metallographic techniques. Scanning electron microscopy (SEM) and electron dispersive spectroscopy (EDS) was used to examine features of the material and the fracture surface. Finally, a mechanics analysis was included in order to calculate an approximation of the actual operating stresses, the critical stress-intensity factor (K_{IC}) for the material, the stress-intensity factor (K_I) under observed conditions, and the possible crack propagation rates under actual loading. Measurements of the residual stress were also taken utilizing X-ray diffraction.

U.S. Army Materials Technology Laboratory
Watertown, Massachusetts 02172-0001
METALLURGICAL EXAMINATION OF A DIAPHRAGM - LOCKUP CLUTCH PISTON - Victor K. Champagne, Jr.

Technical Report MTL TR 88-6, April 1988, 33 pp - illus-tables

AD__________

UNCLASSIFIED
UNLIMITED DISTRIBUTION

Key Words

Clutch Piston
High carbon steels
Failure

A metallurgical examination was performed on a diaphragm - lockup clutch piston which experienced cracking around the inside diameter. The study required reviewing the manufacturing procedures, analyzing the service conditions, and determining the operating stresses induced on the part in service. The extent of cracking was verified by using magnetic particle testing. Material identification and characterization was accomplished by performing mechanical testing, chemical analysis, and metallographic techniques. Scanning electron microscopy (SEM) and electron dispersive spectroscopy (EDS) was used to examine features of the material and the fracture surface. Finally, a mechanics analysis was included in order to calculate an approximation of the actual operating stresses, the critical stress-intensity factor (K_{IC}) for the material, the stress-intensity factor (K_I) under observed conditions, and the possible crack propagation rates under actual loading. Measurements of the residual stress were also taken utilizing X-ray diffraction.

U.S. Army Materials Technology Laboratory
Watertown, Massachusetts 02172-0001
METALLURGICAL EXAMINATION OF A DIAPHRAGM - LOCKUP CLUTCH PISTON - Victor K. Champagne, Jr.

Technical Report MTL TR 88-6, April 1988, 33 pp - illus-tables

AD__________

UNCLASSIFIED
UNLIMITED DISTRIBUTION

Key Words

Clutch Piston
High carbon steels
Failure

A metallurgical examination was performed on a diaphragm - lockup clutch piston which experienced cracking around the inside diameter. The study required reviewing the manufacturing procedures, analyzing the service conditions, and determining the operating stresses induced on the part in service. The extent of cracking was verified by using magnetic particle testing. Material identification and characterization was accomplished by performing mechanical testing, chemical analysis, and metallographic techniques. Scanning electron microscopy (SEM) and electron dispersive spectroscopy (EDS) was used to examine features of the material and the fracture surface. Finally, a mechanics analysis was included in order to calculate an approximation of the actual operating stresses, the critical stress-intensity factor (K_{IC}) for the material, the stress-intensity factor (K_I) under observed conditions, and the possible crack propagation rates under actual loading. Measurements of the residual stress were also taken utilizing X-ray diffraction.

U.S. Army Materials Technology Laboratory
Watertown, Massachusetts 02172-0001
METALLURGICAL EXAMINATION OF A DIAPHRAGM - LOCKUP CLUTCH PISTON - Victor K. Champagne, Jr.

Technical Report MTL TR 88-6, April 1988, 33 pp - illus-tables

AD__________

UNCLASSIFIED
UNLIMITED DISTRIBUTION

Key Words

Clutch Piston
High carbon steels
Failure

A metallurgical examination was performed on a diaphragm - lockup clutch piston which experienced cracking around the inside diameter. The study required reviewing the manufacturing procedures, analyzing the service conditions, and determining the operating stresses induced on the part in service. The extent of cracking was verified by using magnetic particle testing. Material identification and characterization was accomplished by performing mechanical testing, chemical analysis, and metallographic techniques. Scanning electron microscopy (SEM) and electron dispersive spectroscopy (EDS) was used to examine features of the material and the fracture surface. Finally, a mechanics analysis was included in order to calculate an approximation of the actual operating stresses, the critical stress-intensity factor (K_{IC}) for the material, the stress-intensity factor (K_I) under observed conditions, and the possible crack propagation rates under actual loading. Measurements of the residual stress were also taken utilizing X-ray diffraction.

U.S. Army Materials Technology Laboratory
Watertown, Massachusetts 02172-0001
METALLURGICAL EXAMINATION OF A DIAPHRAGM - LOCKUP CLUTCH PISTON - Victor K. Champagne, Jr.

Technical Report MTL TR 88-6, April 1988, 33 pp - illus-tables

AD__________

UNCLASSIFIED
UNLIMITED DISTRIBUTION

Key Words

Clutch Piston
High carbon steels
Failure

A metallurgical examination was performed on a diaphragm - lockup clutch piston which experienced cracking around the inside diameter. The study required reviewing the manufacturing procedures, analyzing the service conditions, and determining the operating stresses induced on the part in service. The extent of cracking was verified by using magnetic particle testing. Material identification and characterization was accomplished by performing mechanical testing, chemical analysis, and metallographic techniques. Scanning electron microscopy (SEM) and electron dispersive spectroscopy (EDS) was used to examine features of the material and the fracture surface. Finally, a mechanics analysis was included in order to calculate an approximation of the actual operating stresses, the critical stress-intensity factor (K_{IC}) for the material, the stress-intensity factor (K_I) under observed conditions, and the possible crack propagation rates under actual loading. Measurements of the residual stress were also taken utilizing X-ray diffraction.

END
DATED
FILM
8-88
DTIC